Available online at www.sciencedirect.com
ScienceDirect
Journal of Power Sources 175 (2008) 419–429
JOURNAL OF POWER SOURCES
www.elsevier.com/locate/jpowsour

On-line fault diagnostic system for proton exchange membrane fuel cells

Luis Alberto M. Riascos [a,*], Marcelo G. Simoes [b], Paulo E. Miyagi [c]

[a] *Federal University of ABC, r. Santa Adelia 166, CEP 09210-170, Santo Andre, Sao Paulo, Brazil*
[b] *Colorado School of Mines, 1500 Illinois St, 80401 Golden, CO, USA*
[c] *Escola Politecnica, University of Sao Paulo, Av. Prof. Mello Moraes 2231, CEP 05508-900, Sao Paulo, Brazil*

Received 3 July 2007; received in revised form 2 September 2007; accepted 3 September 2007
Available online 14 September 2007

Abstract

In this paper, a supervisor system, able to diagnose different types of faults during the operation of a proton exchange membrane fuel cell is introduced. The diagnosis is developed by applying Bayesian networks, which qualify and quantify the cause–effect relationship among the variables of the process. The fault diagnosis is based on the on-line monitoring of variables easy to measure in the machine such as voltage, electric current, and temperature. The equipment is a fuel cell system which can operate even when a fault occurs. The fault effects are based on experiments on the fault tolerant fuel cell, which are reproduced in a fuel cell model. A database of fault records is constructed from the fuel cell model, improving the generation time and avoiding permanent damage to the equipment.

Keywords: Bayesian network; Fault diagnosis; Fuel cell

1. Introduction

Major efforts to reduce greenhouse gas emissions have increased the demand for pollution-free energy sources, in the last few years. Governmental and private-sector investments in R&D, to support a program for clean energy generation including hydrogen-based, are under way.

Fuel cells are electrochemical devices that generate electricity, similar to batteries but which can be continuously fueled. Most recent developments in proton exchange membrane fuel cell (PEMFC) technology have made it the most promising for stationary and mobile applications in the range of up to 200 kW. They are characterized by high efficiency, high power density, no aggression to the environment, no moving parts, and superior reliability and durability.

Under certain pressure, hydrogen (H_2) is supplied into a porous conductive electrode (the anode). The H_2 spreads through the electrode until it reaches the catalytic layer of the anode, where it reacts, separating protons and electrons. The H^+ protons flow through the electrolyte (a solid membrane), and the electrons pass through an external electrical circuit, producing electrical energy. On the other side of the cell, the oxygen (O_2) spreads through the cathode and reaches its catalytic layer; on this layer, the O_2, H^+ protons, and electrons produce liquid water and residual heat as sub-products [1].

Several papers have been published considering the fuel cell (FC) operation in normal conditions; but few of them addressed the FC operation under fault conditions. Faults are events that cannot be ignored in any real machine, and their consideration is essential for improving the operability, flexibility, and autonomy of automatic equipment.

In this paper, a fault diagnostic supervisor was designed to execute on-line diagnosis, which indicates the cause of an incipient fault. The supervisor uses a Bayesian network arrangement to establish the cause–effect relationship, and to calculate the probability of the most likely fault cause. An early alert of an incipient fault allows making decisions to avoid degradation of other components and catastrophic faults in the equipment. A FC model able to reproduce the effects of faults on a fuel cell is generated. The supervisor and the FC model were integrated using the MatLab/SimuLink® environment to confirm the characteristics of this interaction.

* Corresponding author. Tel.: +55 11 49963166; fax: +55 11 30915471.
E-mail address: luis.riascos@ufabc.edu.br (L.A.M. Riascos).

0378-7753/$ – see front matter © 2007 Elsevier B.V. All rights reserved.
doi:10.1016/j.jpowsour.2007.09.010

This paper is organized as follows. In Section 2, the monitoring of the fault tolerant fuel cell (FTFC) is presented. In Section 3, the FC model is introduced. In Section 4, four types of faults in PEMFC are considered: faults in the air fan, faults in the refrigeration system, growth of the fuel crossover, and faults in hydrogen pressure. Section 5 presents a short background of Bayesian networks. Section 6 introduces the fault diagnostic supervisor for PEMFC.

2. The fault tolerant fuel cell (FTFC)

The design of a fault diagnostic supervisor requires the analysis of the operation of a FC in fault conditions; a FTFC was constructed at the PSERC laboratory of the Colorado School of Mines (CSM) [2]. The control system, the sensor system, and the power system compose the FTFC. The control system allows the adjustment of the speed of the air-reaction blower and the refrigeration blower. The sensor system allows monitoring the voltage (V_S), electric current (I_{FC}), temperature, and relative humidity (HR_{out}). The power system is composed by one AvistaLabs cartridge containing four proton exchange membranes (PEM). Also, the control of the FTFC can be executed by microcontrollers (inside the FTFC) or based on PC (using the LabView®). The same LabView® is applied for monitoring the variables and the speed of the blowers. The air for reaction and the air for refrigeration are separated on different routes, which simplifies the monitoring process of some variables.

The FTFC allows the operation (and the monitoring) of the system even when faults occur. Fig. 1 illustrates the monitoring of the FTFC; this figure shows the FTFC, the load, and a desktop computer with the LabView® software executing the monitoring.

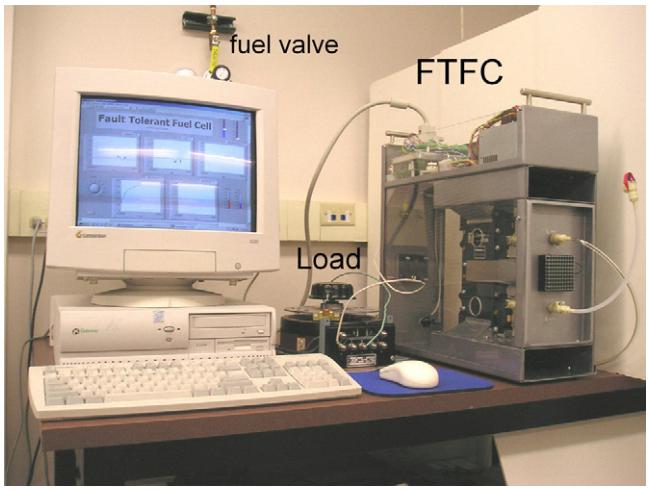

Fig. 1. Monitoring the FTFC.

Fig. 2 illustrates the evolution of several variables such as output stack voltage (V_S), electric current (I_{FC}), temperature, relative humidity (HR_{out}), and airflow volume, using the software LabView®, when the FTFC operates in normal conditions.

The FTFC was tested in different fault conditions. Fig. 3 illustrates the evolution of the output voltage (V_S), electric current (I_{FC}), and relative humidity (HR_{out}) when the H_2 pressure is reduced at $t = 10$ min.

Fig. 4 illustrates the evolution of the output voltage (V_S), electric current (I_{FC}), and relative humidity (HR_{out}) when the air-reaction volume is reduced at $t = 30$ min.

Unfortunately, the generation of each case requires about 2 h of supervised experiments; therefore, the construction of a

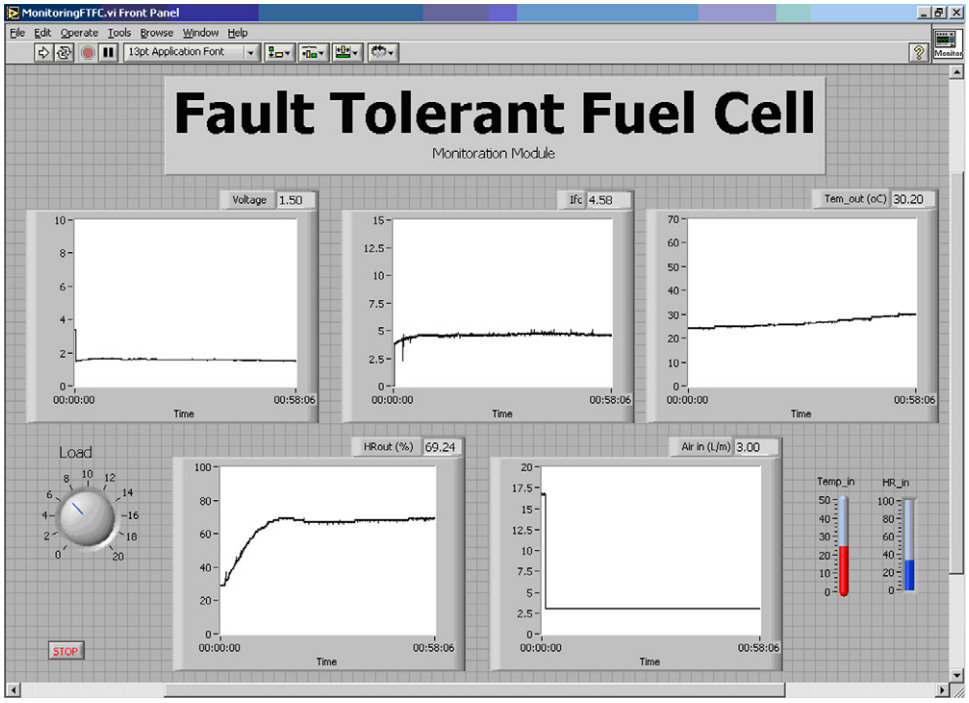

Fig. 2. Evolution of the FTFC's variables in normal conditions.

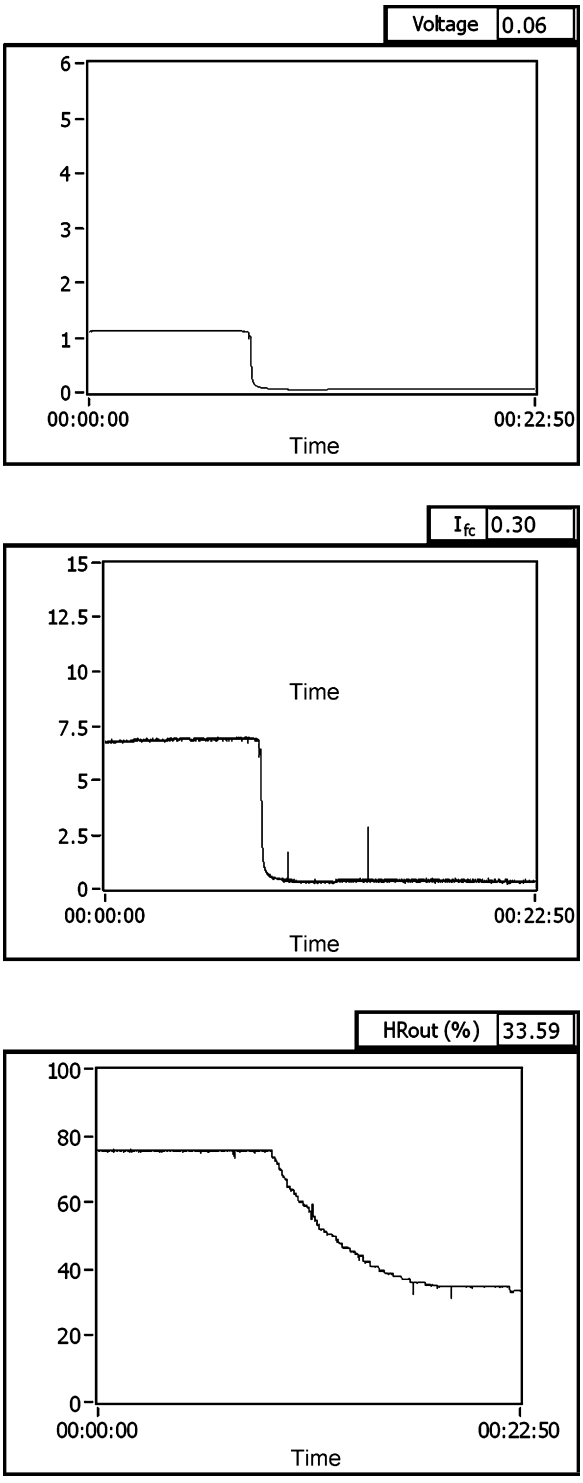

Fig. 3. Evolution of FTFC's variables by reduction of H_2 pressure.

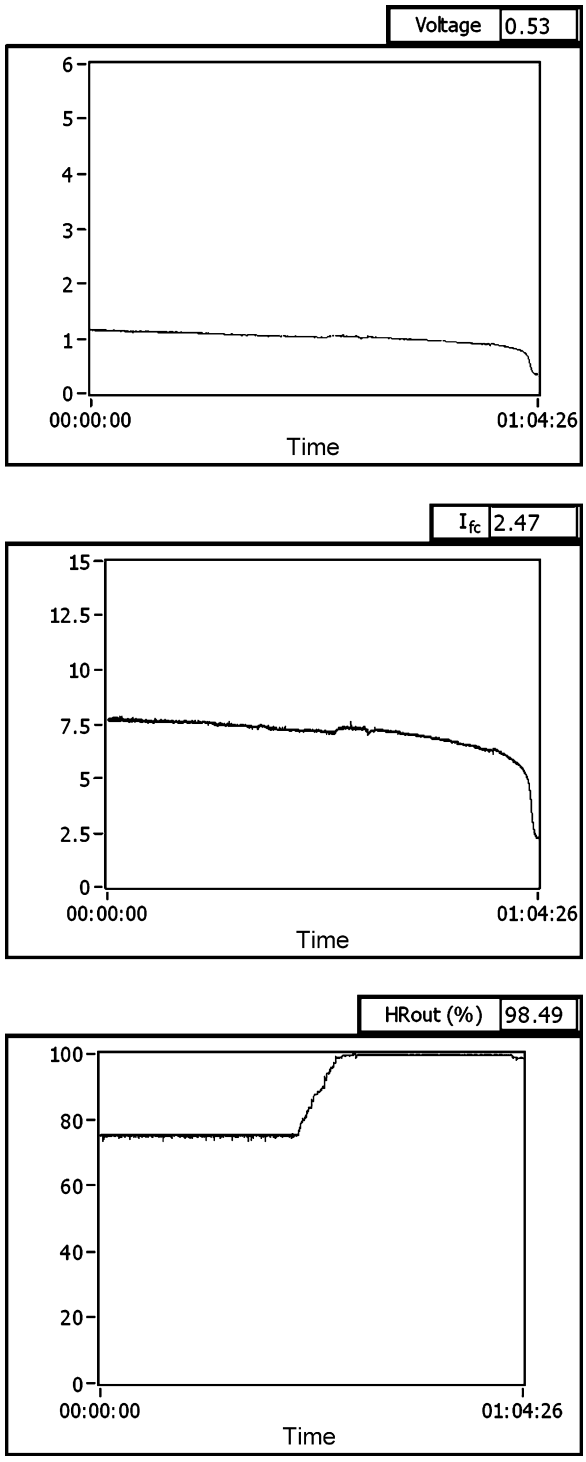

Fig. 4. Evolution of FTFC's variables by reduction of air-reaction volume.

database with a considerable number of cases became highly time-consuming. Also, fault effects such as membrane breaking or dying of membrane imply permanent damage to the FTFC. The effects of different types of faults can be simulated adapting a FC model, avoiding damage to the equipment and improving the generating time of fault records.

3. The fuel cell model

Several mathematical models of PEMFC can be found in the literature [1,3–5]. Basically, a model of PEMFC consists of an electro-chemical and thermo-dynamical parts. Correa et al. [3] introduce an electro-chemical model of a PEMFC; to validate this model, the polarization curve obtained with this model is

compared to the polarization curve of the manufacturing data sheet. In Ref. [6], the thermo-dynamical part of the model and the effects of different types of faults are included.

The FC model is based on the calculation of voltage, temperature, and humidity, according to the equations considered in Ref. [1,3]. The voltage V_{FC} of a single cell can be defined as the result of the following expression [1]:

$$V_{FC} = E_{Nernst} - V_{act} - V_{ohmic} - V_{con} \quad (1)$$

E_{Nernst} is the thermodynamic potential of the cell representing its reversible voltage:

$$E_{Nernst} = 1.229 - 0.85 \times 10^{-3}(T - 298.15) + 4.31 \times 10^{-5} T \left[\ln(P_{H_2}) + \tfrac{1}{2}\ln(P_{O_2})\right] \quad (2)$$

where P_{H_2} and P_{O_2} (atm) are the hydrogen and oxygen pressures, respectively and T (K) is the operating temperature. V_{act} is the voltage drop due to the activation of the anode and the cathode:

$$V_{act} = -[\xi_1 + \xi_2 T + \xi_3 T \ln(c_{O_2}) + \xi_4 T \ln(I_{FC})] \quad (3)$$

where ξ_i ($i = 1 \ldots 4$) are specific coefficients for every type of FC, I_{FC} (A) is electric current, and c_{O_2} (atm) is the oxygen concentration.

V_{ohmic} is the ohmic voltage drop associated with the conduction of protons through the solid electrolyte, and of electrons through the internal electronic resistance:

$$V_{ohmic} = I_{FC}(R_M + R_C) \quad (4)$$

where R_C (Ω) is the contact resistance to electron flow and R_M (Ω) is the resistance to proton transfer through the membrane:

$$R_M = \frac{\rho_M \ell}{A},$$

$$\rho_M = \frac{181.6[1 + 0.03(I_{FC}/A) + 0.062(T/303)^2 (I_{FC}/A)^{2.5}]}{[\psi - 0.634 - 3(I_{FC}/A)] \exp[4.18((T - 303)/T)]} \quad (5)$$

where ρ_M (Ω cm) is the specific resistivity of membrane, ℓ (cm) the thickness of membrane, A (cm^2) the active area of the membrane, and ψ is a coefficient for every type of membrane.

V_{con} represents the voltage drop resulting from the mass transportation effects, which affects the concentration of the reacting gases:

$$V_{con} = -B \ln\left(1 - \frac{J}{J_{max}}\right) \quad (6)$$

where B (V) is a constant depending on the type of FC, J_{max} the maximum electric current density, and J is the electric current density produced by the cell. In general, $J = J_{out} + J_n$ where J_{out} is the real electrical output current density and J_n is the fuel crossover and internal loss current.

Considering a stack composed by several FCs, and as initial approximation, the output stack voltage can be considered as: $V_{Stack} = nr V_{FC}$, where nr is the number of cells composing the stack. However, constructive characteristics of the stack such as flow distribution and heat transfer should be taken [7–11].

The variation of temperature in the FC is obtained with the following differential equation [1]:

$$\frac{dT}{dt} = \frac{\Delta \dot{Q}}{MC_s} \quad (7)$$

where M (kg) is the whole stack mass, C_s (J K^{-1} kg^{-1}) the average specific heat coefficient of the stack, and $\Delta \dot{Q}$ is the rate of heat variation (i.e. the difference between the rate of heat generated by the cell operation and the rate of heat removed). Four types of heat can be removed: heat by the reaction air flowing inside the stack (Q_{rem1}), by the refrigeration system (Q_{rem2}), by water evaporation (Q_{rem3}), and by heat exchanged with the surroundings (Q_{rem4}).

Water forms at the cathode, and because the membrane electrolyte is very thin, water would diffuse from the cathode to the anode during the operation of the cell. The water formation would keep the electrolyte hydrated. This level of hydration is measured through the relative humidity of the output air.

To calculate the relative humidity of the output air, the balance of water is establishes: output = input + internal generation, or in terms of the partial pressure of water: $P_{w_{out}} = P_{W_{in}} + P_{W_{gen}}$.

And, also $HR_{out} P_{sat\_out} = P_{w_{out}}$, then the HR_{out} is

$$HR_{out} = \frac{P_{w_{in}} + P_{w_{gen}}}{P_{sat\_out}} \quad (8)$$

where $P_{w_{in}}$ is the partial pressure of the water in the inlet air, $P_{w_{gen}}$ the partial pressure of the water generated by the chemical reaction, and P_{sat_out} is the saturated vapor pressure in the output air.

The P_{sat} is calculated from the following equation:

$$P_{sat} = T^a \exp\frac{(b/T) + c}{10}$$

If $T > 273.15$ K, then $a = -4.9283$, $b = -6763.28$, and $c = 54.22$;

The rate of water production (kg s^{-1}) is calculated from the next equation [1].

$$\dot{m}_{H_2O} = 9.34 \times 10^{-8} I_{FC}\, nr$$

For normal operation of the FC, proper temperature and humidity should be maintained. If the HR_{out} is much less than 100%, then the membrane dries out and the conductivity decreases. On the other hand, a HR_{out} greater than 100% produces accumulation of liquid water on the electrodes, which become flooded and block the pores, making gas diffusion difficult. The result of these two conditions is a fairly narrow range of normal operating conditions. In abnormal conditions such as flooding or drying, parameters (such as R_C and ψ) that are normally constant (Table 1) start to vary. The parameters of the FTFC model for normal conditions are presented in Table 1.

In general, these parameters are based on manufacturing data and laboratory experiments, and their accuracy can affect the simulation results. In Ref. [12], a multi-parametric sensitivity analysis is performed to define the importance of the accuracy of each parameter. The accuracy was analyzed in normal conditions, considering variations around ±10% of their normal values. However, in fault conditions, those variations can be stronger, as presented in Sections 4.1–4.4.

Table 1
Parameters of the FTFC

Parameter	Value
nr	4
A (cm^2)	62.5
ℓ (μm)	25
P_{O_2} (atm)	0.2095
P_{H_2} (atm)	1.47628
R_C (Ω)	0.003
B (V)	0.015
ξ_1	−0.948
ξ_2	$0.00286 + 0.000\,2\ln A + (4.3 \times 10^{-5})\ln c_{H_2}$
ξ_3	7.22×10^{-5}
ξ_4	-1.06153×10^{-4}
ψ	23.0
J_n (A cm^2)	0.022
$J_{máx}$ (A cm^2)	0.672

In Ref. [13], the water and thermal management in fuel cell systems were analyzed considering extra humidification at the cathode and anode. Forms of extra humidification can include liquid water injection, direct membrane humidification, recycling-humidification and many other methods; in Ref. [14], the parameters that affect the liquid water flux through the membrane and gas diffusion layer are analyzed. In Ref. [15], the dynamic performance of PEMFC is tested under various operating conditions and load changes.

Fig. 5 illustrates the effects of variation in temperature and HR_{out} maintaining constant stoichiometric air relationships ($\lambda = 2, 4, 8$) applying the FC model. The stoichiometry (λ) is the relationship between inlet air divided by the air necessary for the chemical reaction.

To avoid the membrane-drying problem, some researches (e.g. [1,13]) have proposed extra humidification in the input reaction air. However, the variation in the HR of the input air produces a very small adjustment in the output HR; for example, a variation of 10% in the input HR represents a variation of approximately 2% in the output HR. Thus, in many cases, the extra humidification of the input air is not enough to resolve the drying problem. Fig. 6 illustrates the variation produced in the HR output air by the adjustment in the HR input air.

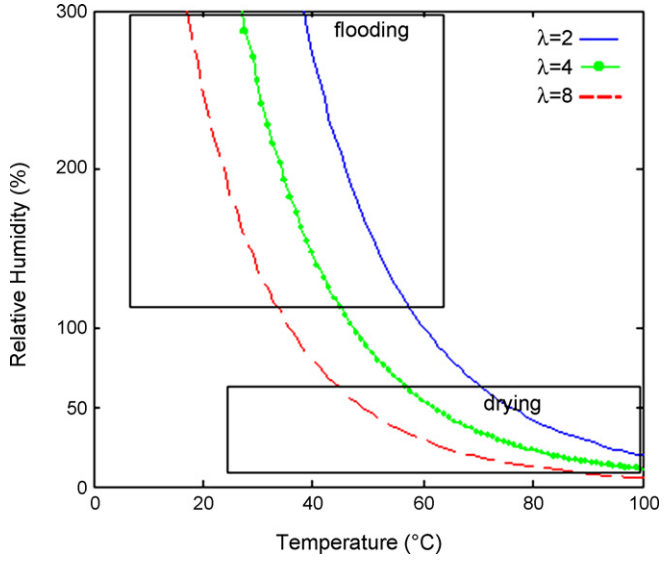

Fig. 5. Temperature and relative humidity HR_{out} for λ = constant.

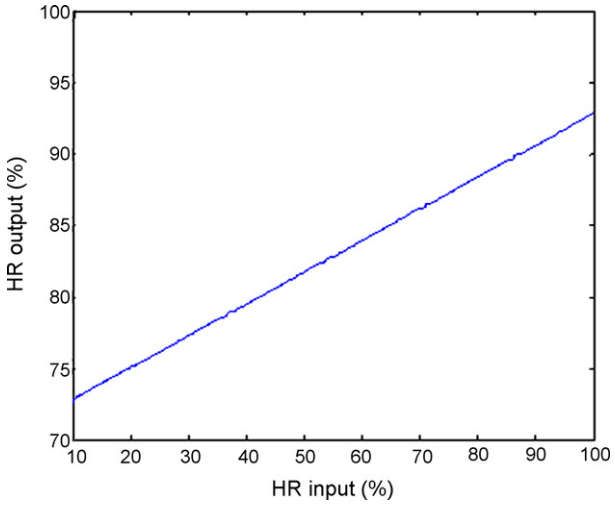

Fig. 6. Variation of output HR by adjusting the input HR.

4. Faults in fuel cells

In general, two categories of fault detection can be considered [16]:

- Faults that can be detected by monitoring a specific variable. For example, fuel leaks can be detected by installing a specific gas sensor. In this case, a diagnosis is not necessary.
- Faults that cannot be detected directly by monitoring or faults that need some type of diagnosis.

In practice, fault detection on commercial FC equipment is limited to detection of faults of the first type. This work focuses on fault detection of the second type.

Four types of faults in PEMFCs are considered in this study: fault in the air blower, fault in the refrigeration system, growth of fuel crossover and internal loss current, and fault in hydrogen pressure. The effects of these faults and the behavior of the FTFC in fault operating conditions are included in the FC model [6].

4.1. Faults in the air-reaction blower

A reduction of the reaction air by a fault in the air blower can produce two major effects: (i) accumulation of liquid water that cannot be evaporated, thus affecting the resistivity of electrodes, and (ii) reduction of O_2 concentration below that necessary for a complete reaction with the H_2.

A common method for removing excess water inside the FC is using the air flowing through it. The correct variation of the stoichiometry λ maintains the HR proximal to 100%. However, when a fault in the air blower takes place, this becomes impossible. This fault reduces the air-reaction flow, which reduces

the water evaporation volume and permits the accumulation of water. A great accumulation of water causes the flooding of electrodes making gas diffusion difficult and affecting the resistance of the electrodes and the performance of the FC. This effect is simulated by the following equation [6]:

$$\mathrm{Rc}_{(k)} = \mathrm{Rc}_{(0)}\left(\frac{w_{\mathrm{accum}(k)}}{\mathrm{const}_1}\right)^{0.8} \tag{9}$$

where $\mathrm{Rc}_{(0)}$ is the value of the variable at the initial state (normal condition), $w_{\mathrm{accum}(k)}$ the volume of water accumulated at instant k, and const_1 is a constant defining when the electrodes are led to flooding.

The second effect of a fault in the air-reaction blower occurs when λ is below the practical and recommended value. In this case, the O_2 concentration is reduced and the exit air completely depleted of O_2. This reduction of O_2 concentration produces a negative effect on the E_{Nernst} (Eq. (2)) and the increment on the V_{act} (Eq. (3)). Fig. 7 illustrates the evolution of output voltage (V_S), electric current (I_{FC}), water volume accumulated, relative humidity ($\mathrm{HR}_{\mathrm{out}}$), and stoichiometry, when a partial fault in the air blower occurs at $t = 30$ min.

4.2. Fault in the refrigeration system

The refrigeration system maintains temperature within operating conditions. When the temperature increases, the reaction air has a drying effect and reduces the relative humidity (HR). A low HR can produce a catastrophic effect on the polymer electrolyte membrane, which not only totally relies upon high water content, but is also very thin (and thus prone to rapid drying out). The drying of the membrane changes the membrane's resistance to proton flow (R_M). R_M is affected by the adjustment of ψ, which varies according to the following equation [6]:

$$\psi_{(k)} = \frac{\psi_{(0)}}{(\mathrm{const}_2/\mathrm{HR}_{\mathrm{out}})^{1.12}} \tag{10}$$

where $\psi_{(0)}$ is the value at the saturated condition (around 100% of HR), $\mathrm{HR}_{\mathrm{out}(k)}$ is the relative humidity of the outlet air at instant k, and const_2 is a constant defining when the membrane is led to drying.

Fig. 8 illustrates the evolution of output voltage (V_S), electric current (I_{FC}), temperature, relative humidity ($\mathrm{HR}_{\mathrm{out}}$), and stoichiometry produced by a fault in the refrigeration system (i.e. a reduction of $Q_{\mathrm{rem}2}$) at $t = 30$ min.

4.3. Increase of fuel crossover (J_n)

There is a small amount of wasted fuel that migrates through the membrane. It is defined as fuel crossover—some hydrogen will diffuse from the anode (through the electrolyte) to the cathode, reacting directly with the oxygen and producing no current for the FC.

In normal conditions, the flow of fuel and electrons through the membrane (J_n) is very small, typically representing only a few mA cm^2. A sudden increase in this parameter can be associated with rupture of the membrane. This variation of J_n produces an increase in the concentration voltage drop (V_{con}, Eq. (6)), and therefore a reduction of V_{FC}. Fig. 9 illustrates the evolution of output voltage (V_S), electric current (I_{FC}), generated heat (Q_{gen}), real output power ($\mathrm{Pot}_{\mathrm{real}}$), and stoichiometry produced by an increase in the fuel crossover (J_n) from 0.022 to 0.2 A cm^2 at $t = 30$ min.

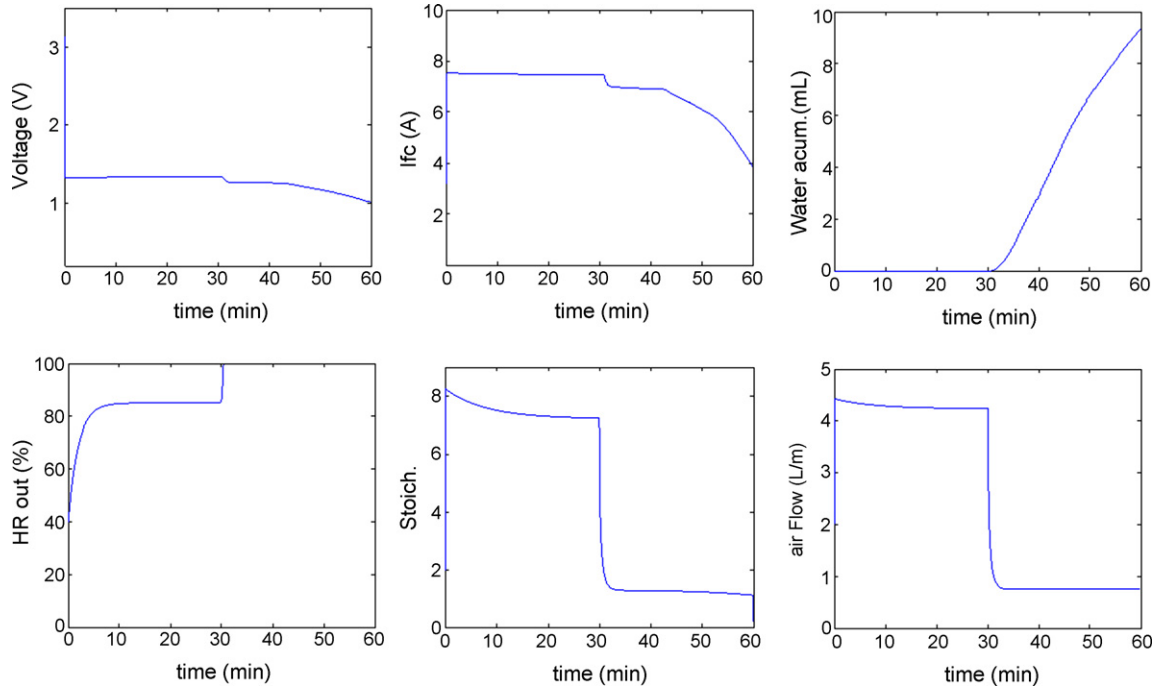

Fig. 7. Evolution of the FC model by air-reaction fault.

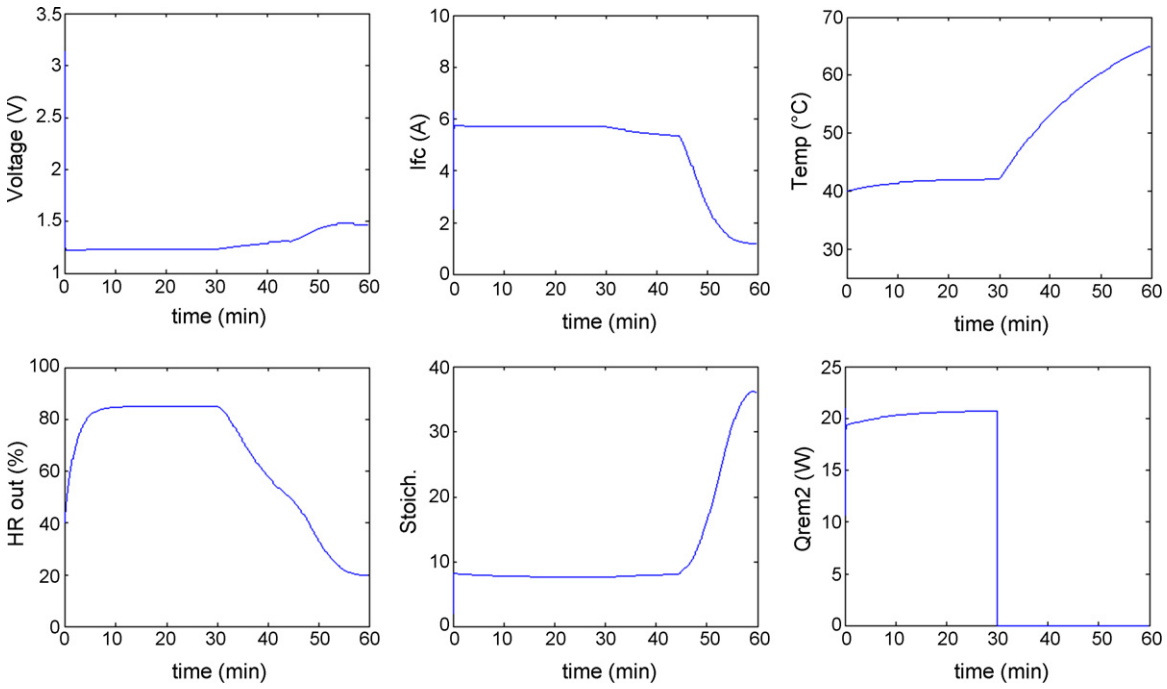

Fig. 8. Evolution of the FC model by refrigeration system fault.

4.4. Fault in hydrogen pressure

In general, for mobile and stationary applications, hydrogen is supplied by a high-pressure bottle, which is reduced by a pressure regulator. In normal conditions, the hydrogen pressure is assumed to be constant (generally between 1 and 3 atm). A lower pressure negatively affects the performance of the FC. The reduction of H_2 pressure decreases the E_{Nernst}, increases the V_{act}, and has a corresponding effect on V_{FC}. Fig. 10 illustrates the evolution of output voltage (V_S), electric current (I_{FC}), generated heat (Q_{gen}), stoichometry, and relative humidity (HR_{out}) produced by a reduction of the H_2 pressure.

In this section, the effects of four types of faults on the FC operation were explained simply and directly. However, when a fault occurs, an interconnected dependence among the variables is established; in general, all the variables perform some kind of

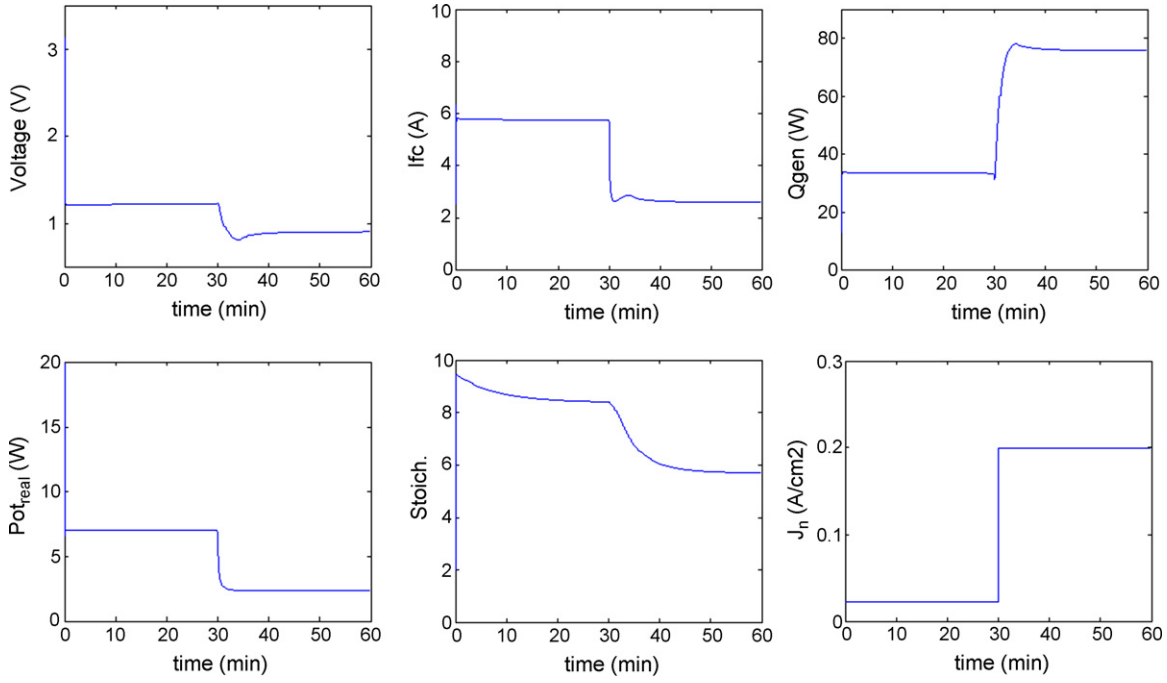

Fig. 9. Evolution of the FC model by membrane breaking.

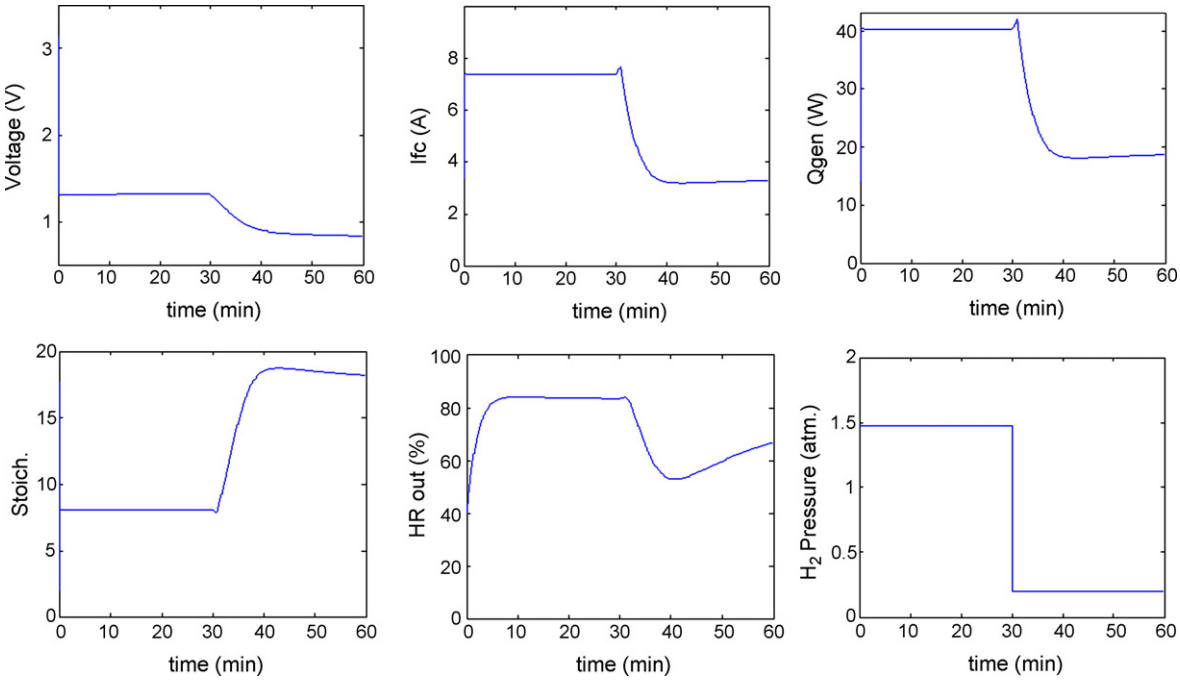

Fig. 10. Evolution of the FC model by H_2 pressure fault.

changes. That hinders the diagnosis of the fault cause. To qualify and quantify the dependence among the variables, a Bayesian network is constructed to conduct the fault diagnosis.

5. Bayesian networks for fault diagnosis

Bayesian networks have been extensively applied to fault diagnosis, e.g. [17,18]; however, in the area of fuel cells, it is a new field. In Ref. [17], a Bayesian network is implemented for controlling an unsupervised fault tolerant system to generate oxygen from the CO_2 on Mars atmosphere. In Ref. [18], Bayesian network is applied for fault diagnosis in a power delivery system. One advantage of Bayesian network is that it allows the combination of expert knowledge of the process and probabilistic theory for the construction of a diagnostic procedure; nevertheless, both are recommended for the construction of a "good" Bayesian network.

A Bayesian network is a structure that graphically models relationships of probabilistic dependence within a group of variables. A Bayesian network B = (G, CP) is composed of the network structure G and the conditional probabilities (CP). A directed acyclic graph (DAG) represents the graphical structure G, where each node of the graph is associated to a variable X_i, and each node has a set of parents pa(X_i). The relationship among variables and parents represents the cause–effect relationship. The conditional probabilities, numerically quantifies this cause–effect relationship [19].

The construction of a Bayesian network for fault diagnosis begins with the collection of fault records and then probabilistic methods are applied for the generation of the cause–effect structure. This process consists of the following steps, described in detail in Ref. [6]:

(a) Construction of the database—the records are provided from the FC model implemented on MatLab®. Field experiments could also provide those records; however, two major problems should be considered: (i) large amounts of data are necessary, where the generation of each case takes around 2 h of supervised experiments and (ii) variables such as Q_{gen}, flooding, λ, etc., impose additional challenges to be monitored.
(b) Implementation of search-and-score algorithms (e.g. the Bayesian-score (K2) [20] and MCMC [21]) to find the initial structure. The probabilistic approaches were implemented using the Bayesian Network Toolbox developed for MatLab® in Ref. [21].
(c) Groups of variables are arranged in layers. Fault causes, sensors, and pattern recognition are considered as layers.
(d) Constraint-based conditions and knowledge are applied for improving the structure.
(e) Calculation of conditional probabilities on the final structure. In this research, the maximum posteriori likelihood algorithm [22] was applied.

5.1. Generation of the database

Binary states of the variables are considered (0 = normal, 1 = abnormal). The general procedure is to monitor a specific variable; if after a fault takes place and the value of such variable is off a certain tolerance band, then a flag should be turned to "1". Fig. 11 represents the range of tolerance and the evolution of the I_{FC} after a fault at $t = 30$ min.

The next step is the construction of a vector containing the value of all variables. This vector corresponds to a single case in the database with values of all variables considered in a cer-

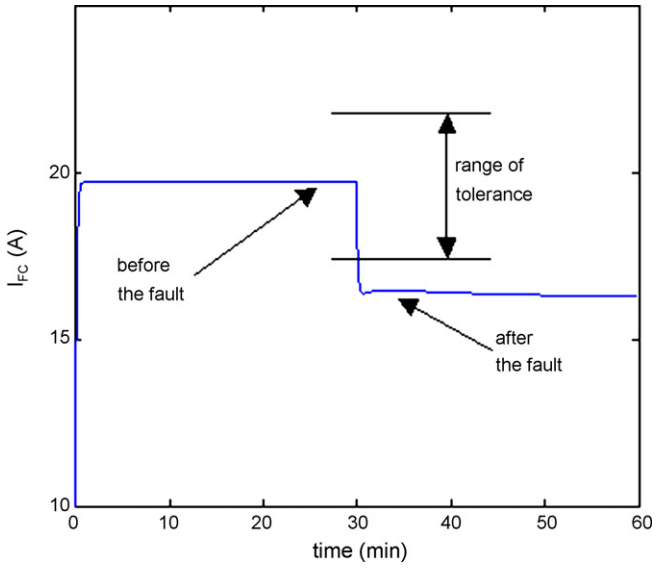

Fig. 11. Evolution of I_{FC} by a fault at $t = 30$ min.

tain period. A database of fault records with 10,000 cases was constructed for the structure learning of a Bayesian network for fault diagnosis in fuel cells. The database considers different operational conditions with different fault causes simulated and selected in a random sequence.

From the mathematical model, the evolution of variables that can be difficult to monitor on a real machine (such as Q_{gen} or λ) can be observed. Records of all variables are essential for the construction of the network structure avoiding hidden variables. The calculation of the diagnosis is simpler if there are no hidden variables [23].

The variables considered are the following:

- J_n = fault by fuel crossover
- aF = fault in the air blower
- rF = fault in the refrigeration system
- H2 = fault by low H_2 pressure
- Fl = volume of air flow
- Q_{gen} = generated heat
- λ = stoichiometric air relationship
- HR = output relative humidity
- Dr = drying of membrane
- Fd = flooding of electrodes
- Ov = overload
- V = voltage$_{stack}$
- I_{FC} = electrical current of the FC
- T = temperature
- Pow = difference between real output power and required load
- P_{H_2} = H_2 pressure

5.2. Search-and-score algorithms

The Bayesian-score (K2) and the Markov Chain Monte Carlo (MCMC) algorithms were implemented in separated ways. The K2 algorithm adds parents to a single node the addition of which most increases the score of the resulting structure. When the addition of no single parent increases the score, it stops adding parents to a node and go to the next node. Before the algorithm begins, the possible parents of every variable must be defined. Therefore, the human-expert experience is important to define that order.

The MCMC algorithm starts at a specific point in the space of all possible DAGs. The search is performed through all the nearest neighbors, and it moves to the neighbor that has the highest score. If no neighbor has a higher score than the current point, a local maximum was reached, and the algorithm stops. A neighbor is the graph that can be generated from the current graph by adding, deleting or reversing a single arc.

In practice, the search-and-score algorithms are not exact, and used only as initial approximations, also since the Bayesian-score and MCMC algorithms applied different tradeoffs for searching the structure, those algorithms can produce different results; therefore, knowledge about the conditional independence among the variables should be applied for obtaining a resulting graph.

5.3. Layers of the Bayesian network

For a better understanding of the relationship among variables, those are separated in several layers. In the final structure, three layers are considered: fault causes, sensors, and pattern recognition. Fault causes are the possible causes of the fault such as fault in the air fan (aF), fault in the refrigeration system (rF), growth of J_n, and low H_2 pressure. Sensors are the variables that can be easily monitored by sensors such as output voltage (V_S), electric current (I_{FC}), power, temperature, and H_2 pressure (P_{H_2}). Pattern recognition is associated with variables difficult to monitor in a real machine, but that play an important role in a cause–effect structure and define a fault pattern. Those variables are: generated heat (Q_{gen}), stoichiometric air relationship (λ), volume of air flow (Fl), drying of membrane (Dr), flooding of electrodes (Fd), overload (Ov) (i.e. the FC is working close to the maximum load—in those cases, some variables perform a different evolution), and relative humidity (HR_{out}) (remember, HR_{out} can only be measured between 0% and 100%).

5.4. Constrain-based conditions and knowledge

First, the fusion of the results applying several probabilistic algorithms confirms the edges present in different structures, second, the remaining edges are submitted to erasing based on constrains and domain knowledge. This process is described in detail in Ref. [6].

Some of the considered constraints are: (i) independent fault cause assumption, i.e. only one fault takes place each time, and one fault cause does not influence other fault cause; (ii) independent sensors—edges among sensors can be erased because their values are always observed.

Fig. 12 illustrates the resulting Bayesian network structure for fault diagnosis in PEMFC. The conditional probabilities (CP) are obtained by the maximum posteriori likelihood algorithm [23] on the network structure considered in Fig. 12. The Bayesian

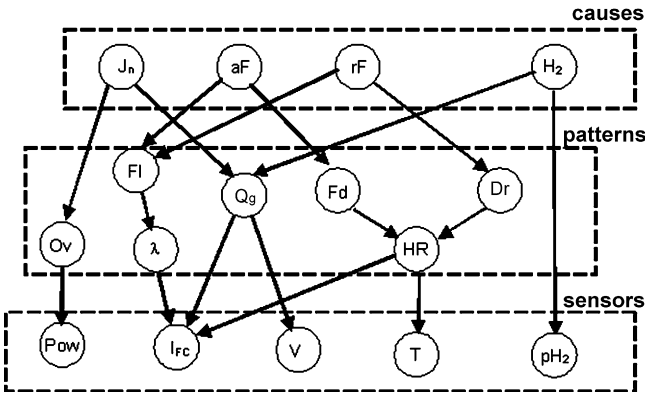

Fig. 12. Bayesian network structure for fault diagnosis in a PEMFC.

network B composed of the network structure G plus CP is ready to be used for fault diagnosis in a PEMFC.

Network structures representing a diagnostic process play a fundamental role for fault tolerant machines since they can be associated with fault treatment processes (i.e. performing the fault diagnosis to identify the fault cause and executing the automatic recovery process). In Refs. [24–26] fault detection and fault treatment were integrated; the case studies were automatic recovery processes in electric autonomous guided vehicles, machining processes and factories.

6. The on-line fault diagnosis

An inference is the computation of a probability $p(X_q|X_E)$, where X_q is the variable of interest (e.g. the most probable fault cause) and X_E is the variable or set of variables that have been observed (i.e. the effects observed by sensors and transformed into logic outputs).

There are many different algorithms for calculating the inference in Bayesian networks, which apply different tradeoffs between speed, complexity, generality, and accuracy. The on-line fault supervisor executes the fault diagnostic inference by applying the variable elimination algorithm, which can be applied to any type of Bayesian network structure [27].

The fault diagnostic fuel cell system is composed of several subsystems: the fuel cell stack and controller, the supervisor, and the peripheryc subsystems. The fuel cell stack contains the electro-chemical and thermo-dynamical parts of the model which calculate voltage, temperature, and humidity. The controller calculates the volume of air-reaction and turns on/off the refrigeration subsystem according to the performance of the process. The supervisor verifies the correct operation of the FC. If monitored variables perform abnormal changes, then the supervisor executes the diagnostic process. The peripheryc subsystems provide the air for the chemical reaction, the hydrogen, the refrigeration, and the load. The environmental conditions are temperature 25 °C and relative humidity 40%.

Fig. 13 illustrates the execution of an on-line fault diagnosis. This test was performed forcing externally the output of the refrigeration subsystem to zero (this simulates a fault condition). In this case, the supervisor detects abnormal variations in

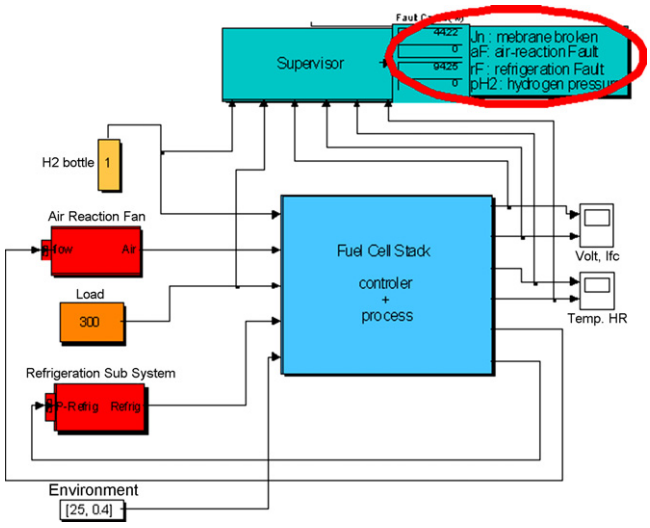

Fig. 13. On-line fault diagnosis execution.

some variables during the operation of the FC. Then, the conditional probabilities were calculated for all fault causes (J_n, aF, rF, and H_2) and shown at the supervisor's display. According to the supervisor, the most probable fault cause is rF (fault in the refrigeration system) with 94% probability. The second probable cause is an increase of J_n with 44% probability. And causes aF and H_2 have 0% probability.

In all tests performed, the supervisor always indicated the true cause as the most probable cause.

In general, the variation of electrical variables (such as output voltage (V_S), and electric current (I_{FC})) is faster than the variation of thermo-dynamical variables (e.g. temperature). Therefore, the diagnosis of faults such as rF takes more time (in this case, around 20 s); actually, this speed depends entirely on the accuracy of the sensors. According to our experience, a worse case scenario still allows fault detection in less than 1 min. But, even 1 min is a good speed for detecting incipient faults before a catastrophic effect takes place in the fuel cell system.

7. Conclusions

The design of a supervisor system to perform on-line fault diagnosis in PEM fuel cells was implemented. The execution of the diagnosis was based on a Bayesian network, which qualifies and quantifies the cause–effect relationship within the variables.

Fault records of some variables were constructed including variables difficult to monitor in a real machine. The record of all relevant variables is essential for the construction of the network structure avoiding hidden variables, especially in intermediary layers.

After the construction of the Bayesian network, the inference calculation is based on observations of variables easy to monitor with sensors such as voltage, electric current, temperature, etc. This allows the implementation of fault diagnostic processes in a real machine.

The fault diagnostic tests have shown agreement between the inference results and the original fault causes.

In general, the fault diagnostic tests were fast enough to detect incipient faults before a catastrophic effect took place in the fuel cell system.

Topics such as the study of fault effects in fuel cells, the construction of network structures for fault diagnosis in fuel cells, and their association to fault treatment processes are still under study, and are still open to research contributions.

Acknowledgments

The authors thank CNPq and FAPESP for financial support.

References

[1] J. Larminie, A. Dicks, Fuel Cell Systems Explained, John Wiley & Sons Ltd., 2003.
[2] L.A.M. Riascos, M.G. Simoes, F.G. Cozman, E. Miyagi, Proceedings of the 41st IEEE-IAS (Ind. Appl. Soc.), Tampa, FL, USA, 2006.
[3] J.M. Correa, F.A. Farret, L.N. Canha, M.G. Simoes, IEEE Trans. Ind. Electron. 51 (5) (2004) 1103–1112.
[4] N. Fouquet, C. Doulet, C. Nouillant, G. Dauphin-Tanguy, B. Ould-Bouamama, J. Power Sources 159 (2) (2006) 905–913.
[5] K. Promislow, B. Wetton, J. Power Sources 150 (4) (2005) 129–135.
[6] L.A.M. Riascos, M.G. Simoes, P.E. Miyagi, J. Power Sources 165 (1) (2007) 267–278.
[7] P.A.C. Chang, J. St-Pierre, J. Stumper, B. Wetton, J. Power Sources 162 (1) (2006) 340–355.
[8] S.A. Freunberger, M. Santis, I.A. Schneider, A. Wokaun, F.N. Büchi, J. Electrochem. Soc. 153 (3) (2006) A396–A405.
[9] S.A. Freunberger, A. Wokaun, F.N. Büchi, J. Electrochem. Soc. 153 (3) (2006) A909–A913.
[10] G.-S. Kim, J. St-Pierre, K. Promislow, B. Wetton, J. Power Sources 152 (1) (2005) 210–217.
[11] M. Santis, S.A. Freunberger, M. Papra, A. Wokaun, F.N. Büchi, J. Power Sources 161 (2) (2006) 1076–1083.
[12] J.M. Correa, F.A. Farret, L.N. Canha, M.G. Simoes, V.A. Popov, IEEE Trans. Energy Conver. 20 (1) (2005) 211–218.
[13] C. Bao, M. Ouyanga, B. Yib, Int. J. Hydrogen Energy 31 (2006) 1040–1057.
[14] Z. Zhan, J. Xiao, D. Li, M. Pan, R. Yuan, J. Power Sources 160 (2) (2006) 1041–1048.
[15] Q. Yan, H. Toghianib, H. Causeya, J. Power Sources 161 (1) (2006) 492–502.
[16] P.M. Frank, Proceedings of International Symposium on AI in Real-time Control, Delft, 1992, pp. 363–370.
[17] U. Lerner, B. Moses, M. Scott, S. McIlraith, D. Koller, Proceedings of 18th Conference on Uncertainty in AI, 2002, pp. 301–310.
[18] C.F. Chien, S.L. Chen, Y.S. Lin, IEEE Trans. Power Delivery 17 (3) (2002) 785–793.
[19] D.M. Chickering, J. Mach. Learn. Res. 3 (2002) 507–554.
[20] G.F. Cooper, E. Herskovits, Mach. Learn. 9 (4) (1992) 309–347.
[21] K. Murphy (2005). http://bnt.sourceforge.net/.
[22] J. Pearl, Causality: Models Reasoning and Inference, Cambridge University Press, 2000.
[23] J. Pearl, Probabilistic Reasoning in Intelligent Systems: Networks of Plausible Inference, Morgan Kaufmann Publ., 1988.
[24] L.A.M. Riascos, F.G. Cozman, P.E. Miyagi, Proceedings of IEEE-ISIE (Int. Symp. Ind. Electron.), Rio de Janeiro, Brazil, 2003.
[25] L.A.M. Riascos, P.E. Miyagi, Proceedings of IEEE-SMC International Conference on Systems, Man and Cybernetics Tucson, 2001, pp. 2528–2533.
[26] P.E. Miyagi, L.A.M. Riascos, Control Eng. Pract. 14 (4) (2006) 397–408.
[27] F.G. Cozman (2001). http://www-2.cs.cmu.edu/∼javabayes/.